BMC Biomedical Engineering

RESEARCH

Open Access

Development and application of a novel multi-channel in vitro electrical stimulator for cellular research

Jorge R. Cibrão[1,2], Miguel Armada[1,2], Marta F. Lima[1,2], André Vidinha-Mira[1,2], Jonas Campos[1,2], Tiffany S. Pinho[1,2], António J. Salgado[1,2], Alar Ainla[3*] and Nuna A. Silva[1,2*]

Abstract

Background Exposure to electric fields affects cell membranes impacting their potential and altering cellular excitability, nerve transmission, or muscle contraction. Furthermore, electric stimulation influences cell communication, migration, proliferation, and differentiation, with potential therapeutic applications. In vitro platforms for electrical stimulation are valuable tools for studying these effects and advancing medical research. In this study, we developed and tested a novel multi-channel in vitro electrical stimulator designed for cellular applications. The device aims to facilitate research on the effects of electrical stimulation (ES) on cellular processes, providing a versatile platform that is easy to reproduce and implement in various laboratory settings.

Methods The stimulator was designed to be simple, cost-effective, and versatile, fitting on standard 12-well plates for parallel experimentation. Extensive testing was conducted to evaluate the performance of the stimulator, including 3D finite element modelling to analyse electric field distribution. Moreover, the stimulator was evaluated in vitro using neuronal and stem cell cultures.

Results Finite element modelling confirmed that the electric field was sufficiently homogeneous within the stimulation zone, though liquid volume affected field strength. A custom controller was developed to program stimulation protocols, ensuring precise and adjustable current delivery up to 160 V/m. ES promoted neurite outgrowth when applied to SH-SY5Y neural cells or to primary spinal cord-derived cells. In human neuronal progenitor cells (hNPCs), ES enhanced neurite growth as well as differentiation into neurons. In adipose stem cells (ASCs), ES altered the secretome, enriching it in molecules that promoted hNPC differentiation into neurons without enhancing neurite growth.

Conclusions Our results highlight the potential of this multi-channel electrical stimulator as a valuable tool for advancing the understanding of ES mechanisms and its therapeutic applications. The simplicity and adaptability of this novel platform make it a promising addition to the toolkit of researchers studying electrical stimulation in cellular models.

*Correspondence:
Alar Ainla
alar.ainla@inl.int
Nuna A. Silva
nunosilva@med.uminho.pt

Full list of author information is available at the end of the article

Keywords Electrical stimulation, In vitro stimulator, Neurite outgrowth, Cellular differentiation, Spinal cord injury

Introduction

Cellular membranes are composed of a lipid bilayer embedded with proteins, among which certain proteins function as ion transporters, commonly known as ion pump proteins. These ion pumps play a crucial role in creating and maintaining concentration gradients within the cell by actively facilitating the movement of selected ions across the membrane. The difference in ionic concentration between the interior and exterior of the cells causes an electrical potential across the membrane (Vm=~-70mV) [1–3]. In neurons and muscle cells, this potential is used for high-speed signal transmission between different parts of the cells and cell-cell communication. These signals are generated by membrane permeability alterations due to the activation or inhibition of both voltage and ligand-gated ion channels. This process induces local changes in ion concentrations within and outside the cells, consequently eliciting a specific shift in membrane potential. This change creates an action potential that will trigger the release of neurotransmitters at the axon terminals. These neurotransmitters will be sensed by ligand-gated channels in the postsynaptic dendrites. This will promote the signal propagation between the cells [4, 5]. Some ions, such as Ca^{2+} are not only responsible for the propagation of electrical signals but also regulate myriad of biochemical -and physical processes inside of the cells.

Upon exposure to an electric field, cell membranes undergo discernible effects impacting its functional processes and influencing its crucial role in maintaining cellular homeostasis. High-intensity electric fields induces electroporation in cells, characterized by the formation of transient pores created by the temporary disruption of the cell membrane. These pores allow the influx and efflux of ions and molecules that would not normally pass through the membrane. This process is widely used in molecular biology techniques for introducing foreign genetic material into cells [1, 2, 6]. The manipulation of the membrane potential is also possible, leading to the activation and inactivation of voltage-gated ion channels, and altering the distribution and concentration gradients of ions, such as potassium, sodium, and calcium. These alterations affect cellular excitability and signalling, leading to consequences on nerve impulse transmission, and muscle contraction [2, 3, 6]. Cell-to-cell communication is also modulated by electric fields, due to modifications on the closing and opening of the gap junctions, which are specialized channels between adjacent cells and play a vital role in the direct exchange of ions and small molecules, thereby affecting intercellular communication and coordination of cellular activities [7]. Moreover, the effects of electrical stimulation (ES) on long-term potentiation (LTP) have been considerably studied. LTP is a process of synaptic plasticity characterized by a long-lasting enhancement in signal transmission between two neurons [8]. Long-term potentiation is the process by which the strength of a synapse increases and is crucial for synaptic plasticity. Mechanistically, electrical stimulation induces long-term potentiation by increasing calcium influx and thereby activating intracellular signaling pathways. These pathways modulate the expression of synaptic proteins and post-synaptic receptors, and amplify synaptic responses [9]. Furthermore, since cells can sense electric gradients, they respond by migrating directionally, either to the anode or the cathode depending on cell type, and proportionally to the electric field strength [10–12]. Cell proliferation and differentiation can also be affected by electrical stimulation [13, 14], with the secretion of FGF-1 and FGF-2 by fibroblast being reported to be significantly upregulated by electrical stimulation, leading to a readjustment in the balance of cell migration, proliferation, and differentiation [15].

Taking this into account, understanding the outcomes of electrical fields on cells is essential to increase our knowledge of fundamental cellular processes. Given its profound effects on cellular function and the fact that cells are programmed to sense and respond to electrical stimulation (ES), this technique has been shown to provide insights into fundamental biological processes, such as gene expression, cellular growth, differentiation, protein synthesis, cell signalling pathways, apoptosis, and cell proliferation [3]. However, the impact of these effects depends on the context, which is influence by factors such as cell type and stimulation parameters. Despite these, the modifications induced by ES may be important for developing new therapeutic strategies. For instance, research indicates that ES leads to elevate levels of neurotrophic factors, such as brain-derived neurotrophic factor (BDNF), glial cell-line derived neurotrophic factor (GDNF), nerve growth factor (NGF), and neuronal cell adhesion molecule (N-CAM), in diverse cells [16–18], suggesting potential therapeutic applications.

In order to study cellular mechanism and effects of electrical stimulation also in combination with chemical one, in vitro stimulation methods are highly useful, due to their simplicity, reproducibility of the conditions and easier access with optical microscopy compared to the in vivo models, as well as due to the ethical considerations. Designing and developing platforms for electrical stimulation in vitro, particularly for cell culture studies, is important because it enables researchers to have access to valuable tools to create more physiologically relevant

models, facilitate mechanistic studies, and pave the way for innovative medical treatments. In this sense, in this work we developed and tested an in vitro electrical platform that is easy to reproduce and adopt for various settings without need for complex instrumentation or tools enabling researchers worldwide to access and utilize the technology to foster advancements in the field of electrical stimulation research.

Materials and methods

Materials of the stimulator

All electronics components were ordered from Digi-Key Electronics (Thief River Falls, Minnesota, US). Printed circuit boards (PCBs) were designed in Eagle (Autodesk Inc, San Francisco, California, US) and ordered from Eurocircuits N.V. (Mechelen, Belgium). Titanium foil (0.35 mm) platinized on both sides (2 µm) was ordered from Goodfellow Ltd. (Huntington, UK) and titanium wire diameter (0.25 mm) from Sigma-Aldrich (Merck KGaG, Darmstadt, Germany).

Finite element modelling

Electric field distribution in the well and the media resistance was analysed using 3D finite element modelling with COMSOL Multiphysics 5.4 (COMSOL AB, Stockholm, Sweden) using electric currents (ec) physics. In order to study influence of the liquid volume and electrode distance from the bottom of the well, these parameters where varied, while remaining were kept constant. Medium was assumed to have linear Ohmic resistance.

Electrical stimulation lid for multiwall plate

2D design of the stimulation lid was prepared in AutoCAD (Autodesk Inc.) and cut into 5 mm thick acrylic (PMMA) sheet using laser engraving system Widlaser LS1390 Plus (Widinnovations Lda, Barcelos, Portugal). Electrodes were cut from the Ti foil mechanically and bent into L-shape and were glued to the acrylic lid using two component epoxy glue. For electrical wiring electrical screw connectors were used. Other ends of the wires were soldered to 3.4 mm 4-pole audio jack connectors.

Electronics

Electronics was designed modularly from two-layer PCBs, which could be stacked together with standard 0.1" pin-headers and sockets. Three types of boards were used, which are described in detail in supplementary information section 1 ("Design of electronic controller"). Components were soldered manually to the PCBs. Field strength for each of the well and the exact timing (durations of negative and positive polarity and delays in between) was programmatically defined by the software of the microcontroller, which was developed in Arduino programming environment.

Evaluation of electric field strength

In order to experimentally test and calibrate the electric field strength, we prepared a test well by mounting two 0.25 mm diameter titanium wires to the bottom of the well using Kapton® tape leaving exposed 7 mm long sections of the wire in the middle of the well. Wires were separated by about 5 mm and tests were performed in Neurobasal Medium with controlled volume (1-2mL) in the well, since both volume and conductivity would affect the field strength. Measurements were performed with 100 MHz digital oscilloscope MSO-X 3014 A (Agilent Technologies Inc. Santa Clara, California, US), where potential and timing was measured directly with the oscilloscope software and traced from the captures of the waveforms from the oscilloscope screen.

Electrical stimulation settings

To assess the effects of in vitro electrical stimulation, three different stimulation protocols were tested. One of the parameters tested, Settings 1 (S1), were described in our lab as an axonal growth inducer in DRGs [19], with an electric field of 25 V/m, a pulse width of 125 ms, and a frequency of 4 Hz. Settings 2 (S2), based on rat's EES values, were also evaluated with an electric field of 150 V/m, a pulse width of 0,5 ms, and a frequency of 200 Hz. The last settings tested, Settings 3 (S3), were based on values used for human EES, with an electric field of 25 V/m, a pulse width of 25 ms, and a frequency of 20 Hz.

In vitro studies

All experiments were previously approved by the Ethical Subcommittee in Life and Health Sciences Institute (ICVS, Braga, Portugal) and Portuguese Authorities (DGAV; ID:022405). Local regulations on animal care and experimentation (European Union Directive 2010/63/EU) were respected. Wistar Han rats (Charles River, USA) were maintained in the Institute of Life and Health Sciences (ICVS, Braga, Portugal) animal facilities under sterile conditions and in light, humidity, and temperature-controlled rooms. Animals had food and water provided ad libitum. For the in vitro studies involving mixed spinal cord cells cultures P5 rat pups were used.

Temperature measurements

Due to the potential of increased temperature caused by the electrical stimulation, temperature was measured for the time points used in the assays (10 and 30 min), before and after each stimulation. This was done using two different media, phosphate-buffered saline (PBS) and Neurobasal-A. The measurements were done using IKA™ Hot Plate Stirrer, 310 °C, Aluminium Alloy with the aid of an included PT 1000 temperature sensor (PT 1000.60).

SH-SY5Y maintenance, culture, and differentiation

SH-SY5Y cells were maintained in Dulbecco's Modified Eagle's medium and incubated in a controlled humidity incubator at 37 °C with 5% CO_2. The cells were treated with Retinoic acid (RA) (10 μM) for one week, to obtain cells with characteristics of mature neurons. After that, cells were seeded on 13 mm glass coverslips coated with poly D-lysine (Sigma-Aldrich, USA) and pig gelatine (Sigma-Aldrich, USA). SH-SY5Y cells were maintained and stimulated according to the protocol. Total cells and neurites were measured, and MTS was performed to assess the viability of the culture upon ES.

Preparation and cultivation of spinal cord cells

P5 Wistar Han rats were used for the cultivation of spinal cord cells, following animal welfare protection protocols. The spinal cord was cut into small pieces (1 mm^2) without dorsal root ganglions (DRGs) and meninges, then transferred into 0.25% trypsin-EDTA solution preheated at 37 °C. For 30 min, tissue is digested and triturated using a sterile Pasteur pipette. Digestion is terminated by adding Plating media (DMEM F12, 10% FBS, 1% penicillin/streptomycin, 2 Mm L-glutamine, and GDNF (10 ng/mL)). To triturate gently the tissue was used sterile fire-polished glass pipettes until it formed a cell suspension. The cell solution was filtered in a 100 μm cell strainer to remove debris. Cells were centrifugated at 100 rpm for 5 min at 4 °C without brakes. Previously, was coated coverslips with PolyD-Lusine and Laminin, to plate the cells for 24 h. The medium is changed for feeding media, that consist of Neurobasal, 2% B27 (Thermo Fisher Scientific, USA), 1% penicillin/streptomycin, 1% L-glutamine (Thermo Fisher Scientific, USA), 2% glucose (Merk, USA) (Fig. 4A). Cells culture was maintained at 37 °C and 5% CO_2, and medium changed every two days.

Human neural progenitor stem cells

Human Neural Stem Cells (hNPCs) obtained from the telencephalon region of 10-week-old foetus were kindly donated by Prof. Leo A. Behie (Dalhousie University, Halifax, Nova Scotia, Canada [20]). These cells were thawed at 37 °C and transferred into a T-25 cm^2 cell culture flask. After two days, the cell sample was mechanically dissociated, in a consistent rhythm approximately 40–50 times, until single–cell suspension was achieved. This suspension was centrifuged at 200 x g for 10 min. The supernatant was discarded. To obtain a count of viable cells, Trypan Blue was used as well as a Neubauer chamber. The cells were seeded in a T-25 cm^2 flask, with a volume of culture medium of 6 mL and density of 1×104 viable cells/cm^2. The culture was incubated at 37 °C and 5% of CO_2 in a humidified incubator. For culture media, Complete NeuroCult™ Proliferation Media was prepared according to the STEMCELL Technologies™ protocol. The prepared medium was then supplemented with the following cytokines: Human Recombinant EGF (Sigma Aldrich, 1:1000) (V/V%), Human Recombinant bFGF (Sigma Aldrich, 1:2000) (V/V%) and Heparin Solution (Sigma Aldrich, 1:1000) (V/V%). The morphology of neurospheres and medium colour changes were monitored daily. The medium was replenished every 2 days, with 1 mL of fresh Complete NeuroCult™ Proliferation Media with cytokines, until the cells were ready for subculture.

hNPCs differentiation with ES exposure

To test the effects of ES on hNPCs differentiation, neurospheres were mechanically dissociated and transferred to differentiation medium consisting of Neurobasal A (Thermo Fisher), 2% B-27 (Thermo Fisher Scientific, USA), 1% Glutamax (Thermo Fisher Scientific, USA), 1% Kanamycin (Kan, Thermo Fisher Scientific, USA) and 0,05% bFGF (Sigma-Aldrich, USA). Then, these were seeded in a 12 well culture plate treated with poli-D-lysin (Sigma-Aldrich, USA) and laminin (Sigma-Aldrich, USA), with a cell density of 60.000 cells per well. The cells were maintained in a 37 °C humid atmosphere with 5% CO_2 in this condition for 24 h. An experiment containing 4 experimental groups was conducted, with two groups not being electrically stimulated, one in media with differentiation factors and one in media without differentiation factors, and two groups being electrically stimulated, one in media with differentiation factors and one in media without differentiation factors. ES was performed 24 h and 48 h post-seeding for 10 min, and 24 h after the second stimulation the cell were fixed for immunocytochemistry.

Adipose stem cells

Adipose Stem Cells (ASCs) were collected from human donors, according to the procedure described by Dubois et al. [21], thawed at fifth passage (P5). Each condition was seeded in cell culture flasks with a density of 4.0×103 cells/cm^2 in serum-free conditions and expanded in MEM medium (Minimum Essential Medium α) (α, GIBCO, USA) supplemented with 10% of Foetal Bovine Serum–FBS (FBS, Invitrogen, USA), 1% Penicillin-Streptomycin (P/S, Invitrogen, USA). Every 3 days the medium was changed, and cells were passed by dissociation with 0.05% trypsin-EDTA (Invitrogen, USA) once 80–90% of cells were confluent. The cells were maintained in a 37 °C humid atmosphere with 5% CO_2.

ASCs secretome collection

ASCs were plated at a density of 12×103 cells/cm^2. After 72 h, the medium was removed, cells were washed 4 times with PBS without Ca^{2+} and Mg^{2+}. For the electrically stimulated group, ASCs were electrically stimulated for 30 min in Neurobasal-A (NbA, Thermo Fisher

Scientific, USA). After stimulation, the medium was replaced and the cells conditioned with 0.74 mL of new Neurobasal-A with 1% Kanamycin (Invitrogen, USA), for 24 h. Following this conditioning period, medium containing the factors secreted by hASCs – conditioned medium or secretome – was collected and stored at – 80 °C to preserve its biological features.

hNPCs differentiation with ASCs secretome

To assess the impact of electrical stimulation on ASC secretome, hNPCs were incubated with secretome from hASCs during 24 h. hASCs secretome was obtained following the protocol mentioned at "ASCs Secretome Collection". Afterwards three groups were defined: NPCs cultured in stimulated ASCs secretome; NPCs cultured in control secretome (no electrical stimulation); and NPCs cultured in negative control containing 98% Neurobasal-A (Thermo Fisher Scientific, USA), 1% Glutamax (Thermo Fisher Scientific, USA) and 1% Penicillin-Streptomycin (Invitrogen, USA).

Immunocytochemistry

In the last day of culture, cells were fixed with 4% paraformaldehyde (PFA, Merk, Germany) for 15 min at room temperature. 0.2% Triton X-100 in PBS (PBS-T) was then used for five minutes to permeabilise the cells, followed by blocking of non-specific antibody binding sites in PBS with 10% FCS (Foetal calf serum, Biochrom, Germany) for one hour. The following primary antibodies were used: BIII tubulin (Neurites, Promega, 1:1000), MAP-2 (Mature Neuronal Marker, Sigma-Aldrich, mouse, 1:500), GAP-43 (Axonal Regeneration Marker, Abcam, rabbit, 1:500), Nestin (Nestin Protein Marker, Sigma-Aldrich, rat, 1:200), Olig2 (Oligodendrocytes, Merk-Millipore, rabbit, 1:500), GFAP (Astrocytes, Sigma-Aldrich, mouse, 1:400), and DCX (Immature Neuronal Marker, Abcam, rabbit, 1:300). All primary antibodies were incubated in PBS with 10% FCS, overnight at 4°C. Cells were then washed three times with PBS, and were incubated, for 15 min, with secondary antibodies Alexa Fluor goat anti-mouse and/or anti-rabbit (1:1000, Thermo Fisher, USA). Imaging was performed in the IX81 fluorescence microscope (Olympus, Germany). Neurites were manually measured using Fiji software (NIH, USA), following the protocol by Kim et al. 2018 [22].

Phalloidin/DAPI staining

ASCs were stained with phalloidin and DAPI were fixed in 4% PFA for 20 min at room temperature. The cells' membranes were then permeabilized with 0.3% Triton X-100 before being rinsed three times with PBS (1x). Following the washes, the cells were treated with a 10% FCS in PBS (1x) solution containing Phalloidin (Sigma-Aldrich, USA, 1:500) and DAPI (Invitrogen, USA, 1:1000) for 30 min at RT. Phalloidin and DAPI staining was done for 45 min.

MTS assays

The medium is removed from the SH-SY5Y and mixed culture cells after seven days in culture. Then is diluted the MTS assay reagent (Promega, USA) in the growing medium of each cell in a ratio of 1 to 4 and incubated for 90 min in a humidified, 5% CO_2 atmosphere at 37 °C. Formazan produced by cellular reduction of MTS was measured in a plate reader at an absorbance of 490 nm. The blank control (growth medium stimulated without cells) was subtracted for the absorbance of each experimental group.

Statistical analysis

The statistical analysis was carried out using GraphPad Prism version 9 (GraphPad Software, USA). Before applying any test, normal distribution was evaluated with Kolmogorov-Smirnov test for normality distribution. If all samples followed a normal distribution, a One-way ANOVA was used followed by the Tukey post-hoc test. The non-param Kruskal-Wallis was used followed by a Dunns' post-hoc test for samples that did not follow a normal distribution. A Mann-Whitney test was done between two samples if one failed a normality test. A T-test was done between two samples if both followed a normal distribution. Differences were considered significant if the p-value was lower than 0.05 (95% confidence level). All data is presented as mean ± standard error of mean (SEM).

Results

Stimulator design

While designing the stimulator, our main goal was to develop a platform, which would be simple and cost-effective, yet easy to use and versatile, allowing parallel experimentation with different pulse protocols, in order to compare and optimize their effects. For multiplexed experiments, multi-well plates are a standard tool used widely in life-science labs. Therefore we have designed the device as a stimulator lid, which could be used on any standard 12-well plate (Fig. 1A, B, D). Such approach has been also used previously by both, academic labs [23, 24], as well as commercial products [25]. Other main considerations of the design were the choice of the stimulation electrodes, their integration into the stimulator lid and the controller electronics.

Electrodes

For the choice of electrodes, an essential characteristics is their electrochemical compatibility and stability, since corrosion products (e.g. metal ions) can severely influence the cell culture and be cytotoxic. This risk would be

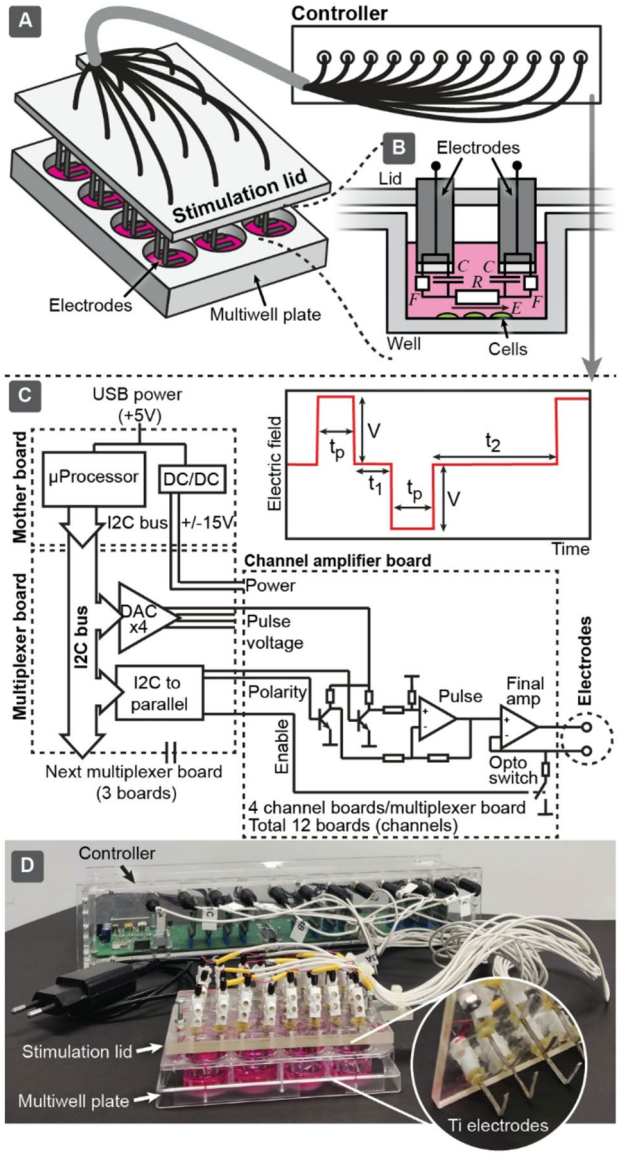

Fig. 1 Design of the in vitro stimulator system. (**A**) Conceptual diagram of the instrument composed of a stimulation lid with electrodes for a multiwell plate, and a stimulation controller. (**B**) In each well two electrodes are submerged into culture medium. Electrically stimulation well can be modelled as ohmic resistance *R*, while electrodes can be represented by capacitive *C* and Faradic *F* elements. (**C**) Conceptual diagram of the stimulation controller, which is designed modularly containing microcontroller and boards to define the pulse shape and individual amplifiers for stimulation pulses in constant current mode. Inset shows bipolar pulse shapes, where electric field and pulse timings can be flexibly defined for each well by the microcontroller firmware. (**D**) Photograph of the in vitro stimulator system composed of controller and stimulation lid with submergible Ti electrodes for usage in the multiwell plate

eliminated by using salt-bridges, but they do suffer from the complexity of their design, requiring individual reservoirs with electrolyte and couplings (e.g. porous frits), which can be prone to bubbles and clogging and changing salt concentrations due to the evaporation, hence needing significant maintenance. Also longer fluidic path between the electrodes means that stimulator electronics has to be driven by higher voltages to achieve the same electric field strength. Therefore, here we have adapted design, where electrodes are directly placed inside of the cell culture chambers (Fig. 2A). Our initial tests with medical grade stainless steel failed due to the corrosion, prompting us to use Pt coated Ti electrodes. Both Pt and Ti have been reported as stable and biocompatible and have been used previously for electrical stimulation electrodes [26–28]. Pt is a good electrode material for aqueous medium, due to the efficient electrochemical splitting of water, which supports stable direct current (DC) through the culture medium without corrosion or alternation of the electrodes, though water splitting itself could produce reactive oxygen species, pH change and gas bubbles. To reduce these effects, a pulse of alternating current (AC) stimulation can be used. Advantages of the Ti is significantly lower cost, thus Pt coated Ti as an electrode material would combine both benefits: stability, cost effectiveness and Faradaic efficiency. We prepared electrodes from a commercial metal sheet, which was first cut into narrow stripes, given L-shape and glued to laser-cut acrylic lid. An important characteristic of the system is the electric field distribution along the cell covered bottom surface of the well and the stability of the field depending on variable input parameters, such as liquid level in the well and height of the electrodes from the surface. In order to characterize it, we performed finite element modelling (Fig. 2B-D), where liquid volume and electrodes height were adjusted, and field strength profile was evaluated. When operated in the constant current mode, the field strength depends only on the properties of the liquid medium, its volume and conductivity, but not on the electrochemical properties of the electrodes. For the first crude estimations of the field strength, we can assume that current distributes homogeneously across the cross-section, of the chamber, in which case the average field strength would be given by the equation $E = I/H_L D_w \sigma$, where parameters are described in the supplementary Table 2. As seen on the Fig. 2B-D, the field, however, does not distribute completely homogeneously. When we compared to the average value from the equation, field strength at the center of the well is 10–20% higher compare to the average. Field is homogeneous in between the electrodes. In order to evaluate the field homogeneity, simulations were carried out by varying the liquid amount and electrode height. When settings ± 10% tolerance threshold from the centre values, we concluded that field was in this homogenous range at least in 4.4 mm x 13.4 mm rectangular area at the center of the well, which we then considered the "Stimulation zone" (Fig. 2B). Height of electrodes from the bottom did not influence significantly the field strength, while liquid

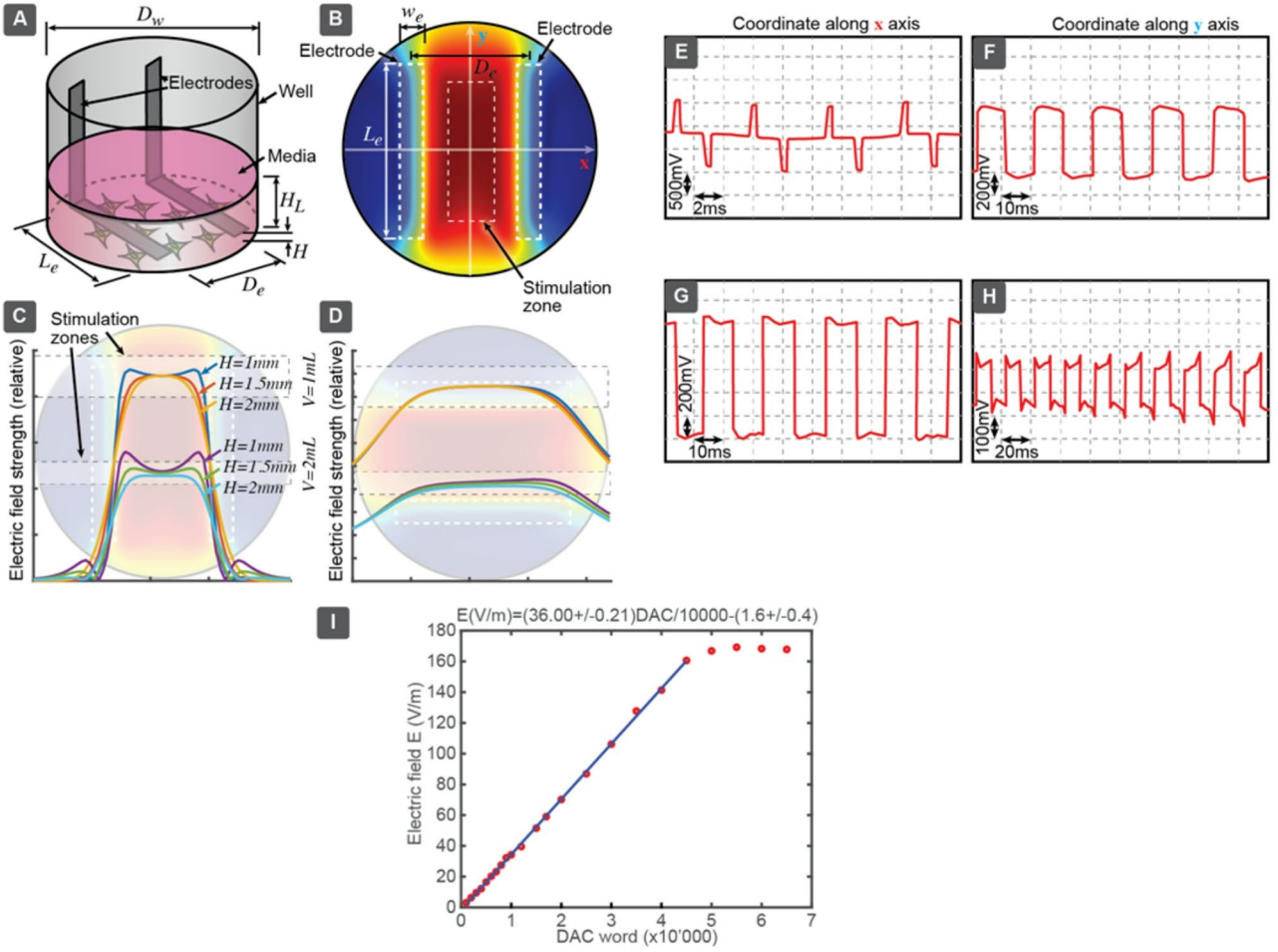

Fig. 2 Finite element modelling of the electric field distribution along the bottom surface of the well. (**A**) Geometrical design of the well. (**B**) Relative electric field distribution, where red represents higher and blue lower field strength. Stimulation zone indicates the region, where field strength is within +/- 10% of the target value. (**C**) Field strength profile along the x axis through the center of the well bottom at different liquid levels corresponding to 1 and 2 mL and electrode heights from the bottom (1, 1.5 and 2 mm). (**D**) Same as previous, but along y axis. (**E**-**I**) Examples of electric field pulse shapes as traced from the screenshots from the oscilloscope. These protocols had following characteristics: (**E**) E = 150 V/m, t_p=0.5ms, t_1 = 1.5ms, t_2 = 2.5ms, f = 200 Hz. (**F**) E = 60 V/m, t_p=10ms, t_1 = 0ms, t_2 = 0ms, f = 50 Hz. (**G**) E = 100 V/m, t_p=10ms, t_1 = 0ms, t_2 = 0ms, f = 50 Hz. (**H**) E = 20 V/m, t_p=10ms, t_1 = 0ms, t_2 = 0ms, f = 50 Hz. (**I**) Calibration of the electric field strength dependence on the DAC defined in firmware code (liquid level ~ 3 mm, corresponding to 1mL volume). Tests and calibrations were performed in Neurobasal Medium

level does, and field is inversely proportional to the liquid volume, as the same electric current would distribute through the larger cross-section yielding lower current density and thus also field strength, while the total current remains constant. Therefore the liquid volume in the wells has to be controlled to maintain the field strength. Also as the field strength would depend on the conductivity $E \propto 1/\sigma$ (Electrical conductivity is known for most commercial media, e.g. see supplementary Table 2). On physiological ionic strength the conductivity is around 1 S/m.

Controller

In order to define stimulation protocols, a suitable electronic control unit is required (Fig. 1C). We considered, that controller should have following features: (i) have individual flexible control for each 12 wells, (ii) stimulations signal would be periodical and composed of equal pulses of opposite polarity and during the idle time the output is electronically disconnected, in order to minimize generation of possible electrochemical reaction products, (iii) pulses are defined by their duration (with 1ms resolution), separating idle time and amplitudes, which all could be changed programmatically and (iv) output is operated at the constant current mode, which would ensure, that electric field pulses are rectangular with well-defined amplitudes. In order to simplify the printed-circuit-boards (PCBs) we divided the design into identical stackable modules (Figs. 1 and 2). Each channel had individual "channel amplifier board" with

analog input signal to set the current, and digital signals to define polarity and enable or disable the output with semiconductor opto-switch (Supplementary Fig. 1, Supplementary Tables 1 and 2). These boards were further connected to the "Multiplexer board", which were stacked and controlled via serial I^2C bus, minimizing the number of required wires (Supplementary Fig. 2). Multiplexer board had digital-to-analog converters (DACs) and serial expander chips to set the state of each channel (Supplementary Tables 3 and 4). I^2C bus was interfaced with master microcontroller, loaded with firmware to define programmatically the stimulation signals for each of the wells (Supplementary Fig. 3, Supplementary Table 5). Since firmware was designed in Arduino language (Supplementary Firmware Code), it would be compatible with all Arduino microcontrollers supporting I^2C operating at 3.3 V logic levels and easy to adapt and modify to add features. We have included detailed circuitry, list of extra components (Supplementary Table 6), device costs (Supplementary Table 7), functional descriptions and exemplary firmware code here to facilitate adaptation and further modifications of this system by the research community. Each channel can be programmed to apply a distinct stimulation protocol to each of the 12 wells (see Supplementary Table 8). Examples of the electric field profile and the corresponding electrical potential on the stimulation electrodes are provided in Supplementary Figs. 4 and 5.

System performance

Besides simulations we tested and characterized the electrical performance of the system by a test well equipped with sensing electrodes, with which we could calibrate the actual pulse shapes and field strengths. The available current would be limited by following factors: (i) output current capability of the operation amplifier (IC2 in Fig. 1, table S1. In case of AD820R the maximum output current is 15 mA), (ii) gain resistor $R_9 = 330\Omega$ (Fig. 1, table S1), (iii) available potential range (IC2 rails), which is ± 15 V, (iv) liquid resistance in the cell (from simulations we found, that liquid resistance was 166Ω and 100Ω for 1mL and 2mL media volumes respectively), (v) electrochemical characteristics of electrodes (voltage drop on electrodes). The maximum current that system can generate is $I = V_{in}/R_9$, which with 3.3 V control signal gives maximum current limit 10 mA. 10 mA would give a potential loss on the media 1–1.7 V in the volume range 1-2mL, this gives still 10 V reserve that amplifier can deliver to electrodes to drive the current (supported either by capacitive or Faradaic currents). In case electrode potential would need to exceed this to maintain the current, controller would saturate the output potential and signal would be distorted. Our tests showed that constant current mode allowed effective delivery of square shaped electric field pulses and (Fig. 2E-H) and potential could be flexibly adjusted in the range up to 160 V/m (Fig. 2I).

Exploring the effects of electrical stimulation on neurite outgrowth

Before performing any cell experiment, we assessed if electrical stimulation had some effects on culture media. To do this, we measured the media temperature at 10 and 30 min of stimulation with no difference being observed between control and the electrical stimulated group (Supplementary Fig. 6). The media pH was also analysed for electrical stimulation-mediated changes, which can be easily detected by observing colour changes in the media. After electrical stimulation no changes in the colour were observed.

We initiate the analysis of the impact of electric stimulation using a neuroblastoma cell line (Fig. 3A) and three different stimulation protocols (Fig. 3B). Evaluation of metabolic activity was assessed through MTS assay and neurite outgrowth through immunoimaging (Fig. 3C). Results revealed no statistical differences or influence of ES on cell metabolic activity (Fig. 3D). This finding suggest that ES does not alter the cellular viability when it is applied for 10 min in neurons. Two days post-ES, cell quantification unveiled a significant increase in the number of cells across stimulated conditions. The total cell counts in the unstimulated group was 138.7 ± 11.44, while the stimulated groups achieve significant higher number of total cells, ES1 (218.6 ± 22.05), ES2 (266.3 ± 25.04), and ES3 (235.9 ± 20.16) (Fig. 3E).

To analyse the effect of ES on neurite outgrowth, we measure the length of neurites in each neuron. Results demonstrated that ES1 and ES2 significantly promote axonal growth when compared to unstimulated cells ($p = 0.0186$ and $p < 0.0001$, respectively), while stimulation with ES3 ($p = 0.0023$) remains lower than the rest groups (Fig. 3F).

Electrical stimulation enhances neural plasticity of spinal cord cells in vitro

P5 rat pups were used to obtain primary cultures of the spinal cord cells (Fig. 4A). These cultures present a diverse array of cells, such as astrocytes, oligodendrocytes, neurons, and progenitors' cells. These cultures were stimulated for 30 min on days five and six of culture in vitro. At seven div, cells were analysed either by immunocytochemistry or by MTS assay.

We first assessed the effect of ES on metabolic activity and on the oligodendrocytes, astrocytes, and progenitors' cells. The MTS test revealed that all stimulated cells present a significantly lower metabolic activity when compared to non-stimulated cells (ES1: $p = 0.0073$; ES2: $p = 0.0002$; ES3: $p < 0.0001$) (Fig. 4B). Despite MTS

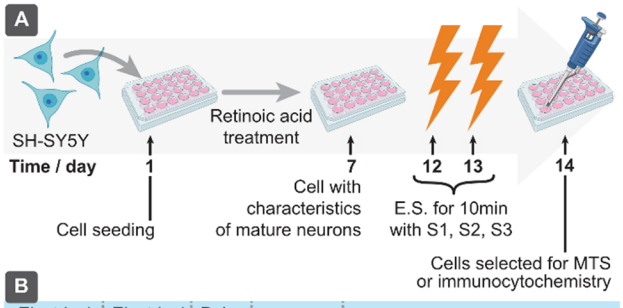

B

Electrical Stimulation Settings	Electrical Field (V/m)	Pulse Width (ms)	Frequency (Hz)	Description
S1	25	125	4	Described before in our lab as an inducer of axonal growth in DRGs
S2	150	0.5	200	Design based on the rat's EES settings
S3	25	25	20	Design based on the human EES settings

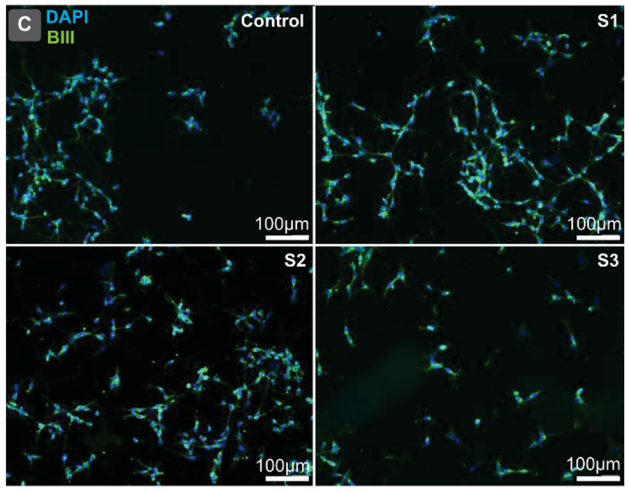

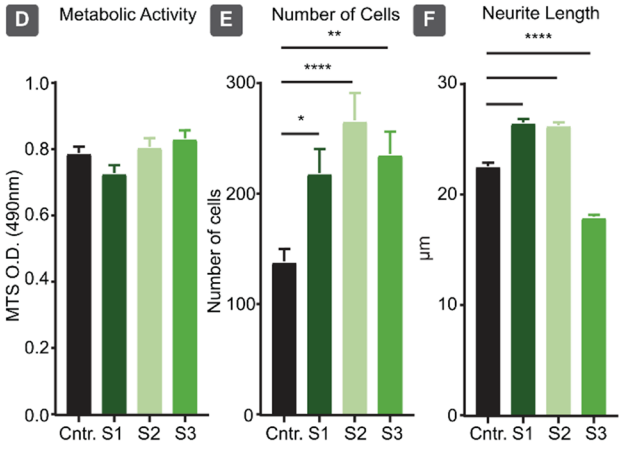

Fig. 3 Different electrical stimulation settings impact SH-SY5Y neuronal cells. (**A**) Diagram of experimental design – Effect of Electrical Stimulation on SH-S5Y5. Cells were cultured for 12 days to allow differentiation into neurons and were then stimulated for 10 min on two consecutive days. After 14 days, the cells were either fixed for immunoimaging analysis or their metabolic activity was assessed using the MTS assay. (Image created with Biorender). (**B**) In vitro electrical stimulator settings. (**C**) Representative fluorescent microscopy images of SH-SY5Y cells, electrical stimulated and non-stimulated, neurites stained with BIII tubulin (green) and nuclei with dapi (blue). (**D**) Metabolic assessment of the cell cultures by MTS assay. (**E**) Cell number quantification at day seven. (**F**) Quantification of the individual cell neurite length. Two independent experiments, $n = 8$. Data are show as mean ± SEM. *p value < 0,05; **p value < 0,01; ****p value < 0,0001. Scale bar: 40 µm

results, we did not observe differences in the total number of cells between the control and the ES1 and ES2 condition. However, ES3 exhibited a significant reduction in total cell number compared to the control ($p = 0.0446$) (Fig. 4C).

In order to comprehend the impact of ES on axonal outgrowth, we conducted an analysis of the neurite length on neuronal populations (Fig. 4D). The results revealed a significant higher neurite outgrowth in ES groups when compared to the non-stimulated group except for the ES2 stimulation setting (ES1: $p = 0.022$; ES2: $p = 0.9988$; ES3: $p < 0.0001$). We also analysed the percentage of neurons within the cultures and observed that electrical stimulation (ES) significantly reduced the percentage of neurons under conditions S2 and S3. In contrast, condition S1 did not show a statistically significant difference compared to the control (Supplementary Fig. 7).

Subsequently, we explored how electrical stimulation influence specific spinal cord cell populations. For that, we quantified the positive areas for GFAP and Nestin, along with the percentage of cells positive for Oligo-2 (Fig. 4E-G). GFAP is a cytoskeleton protein mostly restricted to the astroglial cell bodies and their branches [29]. In the early development stages of the nervous system, Nestin is expressed in dividing cells as an intermediate filament protein. Nestin expression is decreased as cell fate is determined [30, 31]. The Oligo-2 is a nuclear transcription factor expressed in the oligodendrocyte lineage cells. Contrarily, the results of GFAP and Nestin

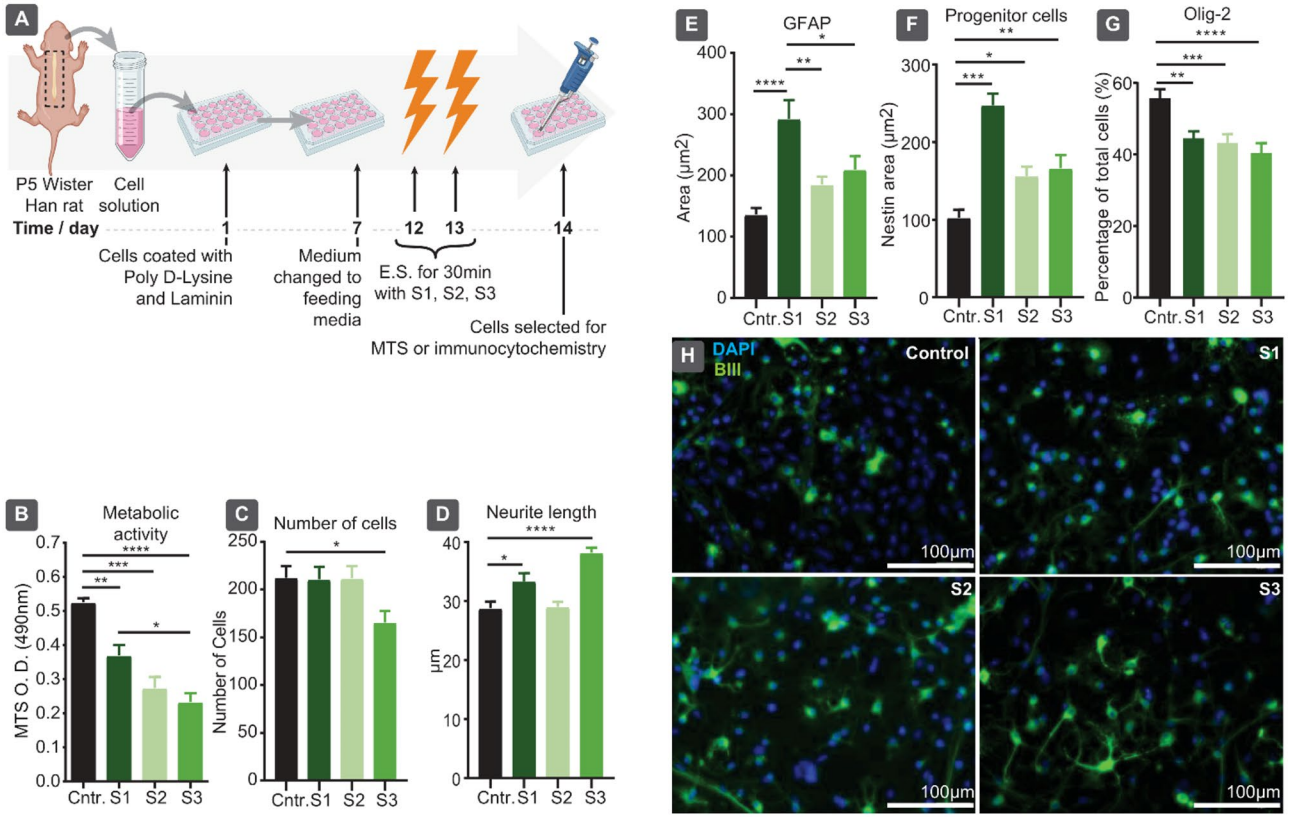

Fig. 4 Electrical stimulation induces cellular and neuronal morphology changes. (**A**) Diagram of experimental design – Effect of Electrical Stimulation on mixed cell culture. Cells were cultured for 12 days and were then stimulated for 30 min on two consecutive days. After 14 days, the cells were either fixed for immunoimaging analysis or their metabolic activity was assessed using the MTS assay. (Image created with Biorender). (**B**) MTS to evaluate the metabolic status of the culture. (**C**) Total number of cells. (**D**) Neurite length was measured manually for each neuron. (**E**) The total area occupied by GFAP positive area normalized for the total cells. (**F**) The total area occupied by Nestin positive area normalized for the total cells. (**G**) Quantification of the percentage of Oligo-2 positive cells relative to total cells. (**H**) Representative immunofluorescence images of primary cultures of spinal cord cells at day 7 for BIII tubulin. $n = 8$. Scale bar: 50 µm. *p value < 0,05; **p value < 0,01; ***p value < 0.001; ****p value < 0,0001; Data are show as mean ± SEM

positive areas followed an inversive tendency (Fig. 4E and F). When ES is given to the cells, both GFAP and Nestin positive area is increased when compared to the unstimulated group (Fig. 4E and F), however for the GFAP area this only happened when applying the ES1 setting, while the positive area for Nestin significantly increased in all ES settings but was more pronounced in the ES1. When ES was applied to the cells, no differences in the percentage of GFAP cells were observed between the experimental groups (Supplementary Fig. 7). Contrarily, when cells were subjected to electrical stimulation, the percentage of cells positive for Oligo-2 were significantly reduced compared to non-stimulated cells (ES1: $p = 0.0021$; ES2: $p = 0.0006$; ES3: $p < 0.0001$) (Fig. 4G). Representative imagens of neurite outgrowth after ES are shown on Fig. 4H.

Effect of electric stimulation on human neuronal progenitor cells

We assessed the effect of ES on the expression of neuronal markers on hNPCs by immunostaining for mature neurons (MAP-2), thus we also analysed axonal growth using GAP-43 marker (Fig. 5C and H). Two cultured conditions were used, hNPCs cultured without differentiation factors or cultured with the differentiation factors 2% B27 and 0,05% bFGF (Fig. 5A and B). Due to the differences observed in the percentage of neurons on spinal cord primary cells, we decided to stimulate the cells for just 10 min instead of the 30 min used before and only used the setting 1. The number of cells was obtained by quantification of DAPI + marked neurons. We then calculated the population obtained for %GAP-43 + and %MAP-2 + cells with the number of GAP-43 + and MAP-2 + cells relative to the total number of DAPI + cells. The mean neurite length per neuron refers to the length of each neurite, from the soma to the end of a bifurcation, marked morphologically by MAP-2. Since no significant difference was observed in the total number of DAPI + cells in each group ($p = 0.1714$ and $p = 0.1123$) (Fig. 5D and I), we can assume that the electrical did not influenced the proliferation of the cells.

Regarding the effects on differentiation and neuronal plasticity, in the hNPCs cultured without differentiation

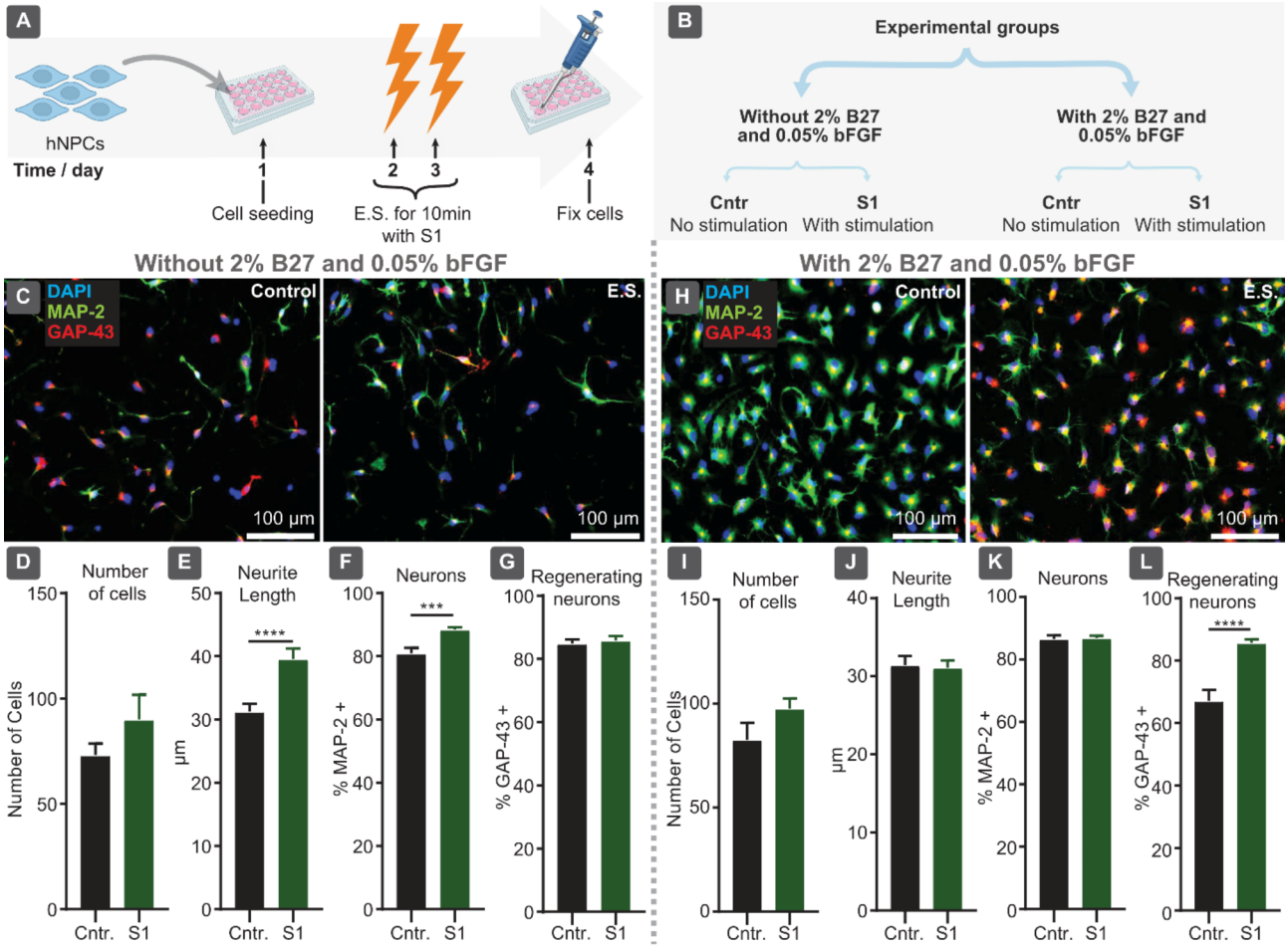

Fig. 5 Electrically stimulated hNPCs with and without growth factors. (**A**-**B**) Diagram of experimental design and experimental groups- Effect of ES on hNPCs. Cells were expanded in neurospheres and then dissociated and cultured in differentiation medium for 2 days, then they were stimulated for 10 min on two consecutive days. After 4 days, the cells were fixed for immunoimaging analysis, (Image created with Biorender). (**C**) Representative fluorescence microscopy images of hNPCs when electrically stimulated and cultured without growth factors. (**D**) Represents the population of DAPI + cells without growth factors. (**E**) Represents the mean neurite length per neuron without growth factors. (**F**) Represents the population of MAP-2 + cells relative to the population of DAPI + cells without growth factors. (**G**) Represents the population of GAP-43 + cells relative to the population of DAPI + cells without growth factors. (**H**) Representative fluorescence microscopy images of hNPCs when electrically stimulated and cultured with growth factors. (**I**) Represents the population of DAPI + cells with growth factors. (**J**) Represents the mean neurite length per neuron with growth factors. (**K**) Represents the population of MAP-2 + cells relative to the population of DAPI + cells with growth factors. (**L**) Represents the population of GAP-43 + cells relative to the population of DAPI + cells with growth factors. ***p value < 0,001; ****p value < 0,0001. Data are show as mean ± SEM. Scale bar: 50 µm

factors, the mean neurite length per neuron was statistically different ($p < 0.0001$) in the cells that were electrically stimulated (Fig. 5E). Statistical difference was also found between non-stimulated and stimulated cells for the %MAP-2+ ($p = 0.0009$) (Fig. 5F). In both conditions, the expression of GAP-43 is high (~ 80%) (Fig. 5G), but no significant differences were observed between groups.

In the presence of differentiation factors, no statistically significant difference was observed between stimulated or non-stimulated hNPCs concerning mean neurite length per neuron ($p = 0.6049$) (Fig. 5J). This finding suggest that the presence of differentiation factors might mitigate the neurite length growth induced by the electrical stimulation. In terms of %MAP-2 + cells, no statistical difference was found between the control and ES ($p = 0.7668$) (Fig. 5K). Only the % of GAP-43 + cells was statistically different between control and ES groups in the presence of differentiation factors ($p < 0.0001$) (Fig. 5L). These results imply that, for inducing neuronal maturation, the presence of differentiation factors alone appears to be sufficient, with the electrical stimulation not having enough power to cause a significant change. However, when differentiation factors are absent, electrical stimulation foster a greater number of cells expressing markers of mature neurons as well as higher neurite growth.

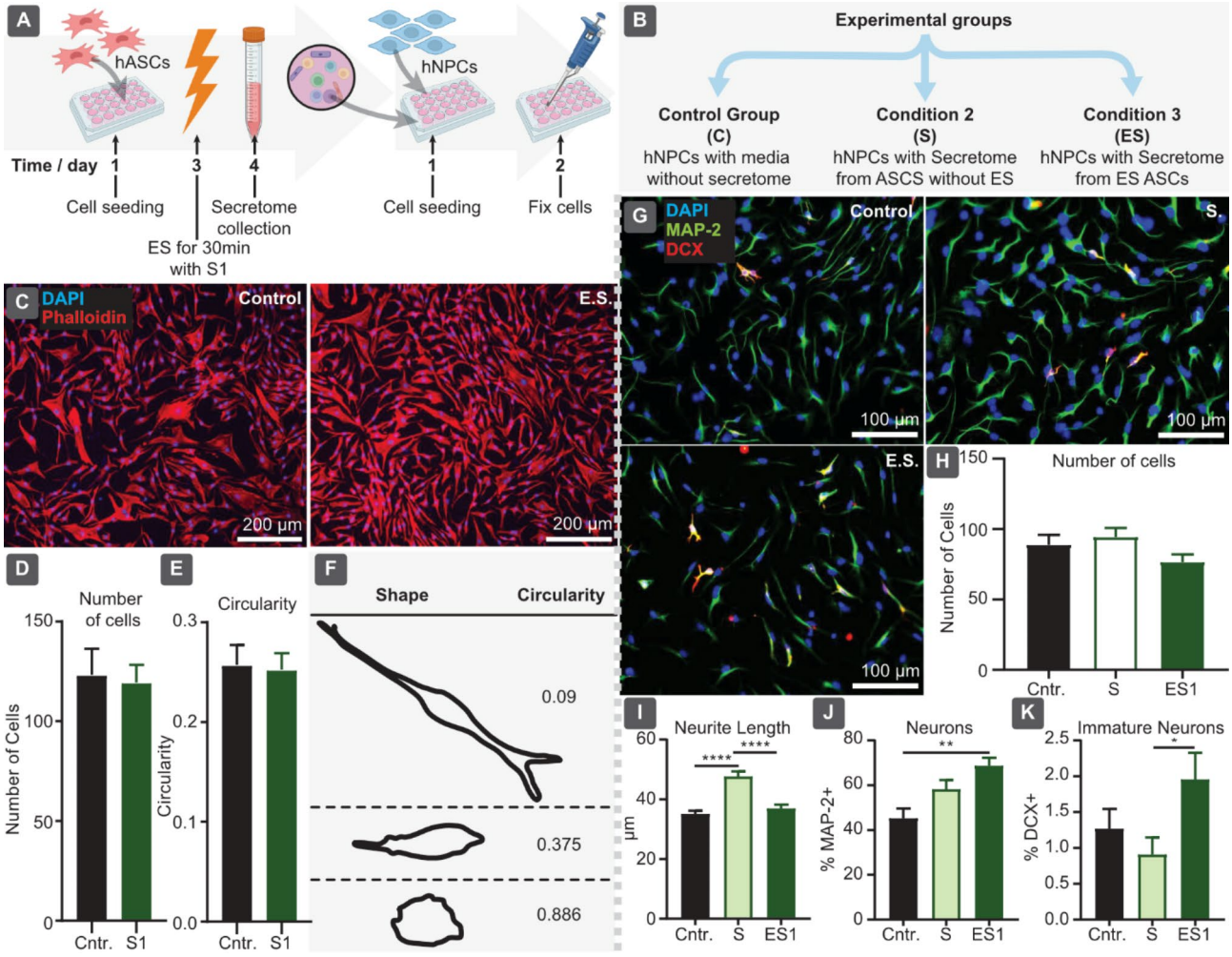

Fig. 6 Effect of Electrical stimulation on ASCs and their secretome on hNPCs. (**A**-**B**) Diagram of Experimental Design and Groups - Effect of Secretome from Electrically Stimulated ASCs on hNPCs. ASCs were cultured until reaching 80% of confluence and them electrically stimulated for 30 min. Then ASCs were allowed to grow for 24 h in serum-free medium for collecting the conditioned medium. The secretome of ASCs were then incubated with hNPCs for 24 h, and cells were then fixed for immunoimaging analysis. (Image created with Biorender). (**C**) Representative fluorescence microscopy images of ASCs when electrically stimulated and control group. Scale bar: 100 µm. (**D**) Represents the population of DAPI + cells. (**E**) Represents the circularity of the cells based on the morphology of phalloidin staining. (**F**) Correlation between shape and circularity of cells. (**G**) Representative fluorescence microscopy images of hNPCs when incubated with secretome from electrically stimulated ASCs. Scale bar: 50 µm. (**H**) Represents the population of DAPI + cells. (**I**) Represents the average neurite length per neuron. (**J**) Represents the population of MAP-2 + cells relative to the population of DAPI + cells. (**K**) Represents the population of DCX + cells relative to the population of DAPI + cells. 'S' denotes the group with non-stimulated secretome. 'ES' denotes the group that was electrically stimulated. **p* value < 0,05; ***p* value < 0,01; *****p* value < 0,0001. Data are show as mean ± SEM

Effect of electric stimulation on human adipose stem cells

After 3 days in culture, ASCs were electrically stimulated for 30 min using the settings ES1 (Fig. 6A). Basal cultured medium (without FBS) was then conditioned with the factors secreted by stimulated or non-stimulated ASCs for 24 h (Fig. 6B). After secretome collection, the cells were marked with phalloidin and DAPI for further analysis (Fig. 6C). The number of DAPI + cells was not statistically different ($p = 0.8064$) (Fig. 6D), showing that cell proliferation was not influenced by ES. The effects of ES on the ASCs morphology were also tested by calculating the circularity for each ASC, using phalloidin to stain the cytoplasm of the cells (Fig. 6E). Circularity is a relation between the area and perimeter, where the closer the value of circularity is to 1.0, the more circular is the shape (Fig. 6F). The typical morphology of ASCs is spindle-shaped, corresponding to a low circularity value. Our analysis demonstrated that the average value of circularity is around 0.25 with no statistical difference in both groups ($p = 0.8918$) (Fig. 6E), showing that the morphology of ASCs remains unaltered by ES.

The effect of ES on the secretory profile of ASCs was assessed by incubating the secretome of these cells with hNPCs (Fig. 6A). Immunostaining was used to assess the expression of neuronal markers on hNPCs, with DCX and MAP-2 for early and mature neurons, respectively.

Moreover, average neurite length per neuron was measured using the MAP-2 immunostaining (Fig. 6G).

The total number of DAPI + cells showed no significant difference between the groups ($p = 0.1021$) (Fig. 6H), suggesting that the stimulated secretome did not influence the proliferation or survival of hNPCs. However, when analysing the average neurite length, and the expression of neuronal markers on hNPCs, it was possible to observe that the ES stimulation significantly alter the secretome of ASCs. For instance, it was possible to observed that the secretome of electrical stimulated ASCs has significant less capability of promoting neurite outgrowth (Fig. 6I). On the other hand, the secretome of electrically stimulated ASCs presented a higher ability to promote the expression of neuronal markers on hNPCs. Results demonstrated that only hNPCs subjected to ES present significantly differences ($p = 0.0015$) on the percentage of mature neurons (MAP-2 + cells) when compared with the control groups (Fig. 6J). Moreover, ES-derived secretome also lead to an increase in the immature neurons in culture ($p = 0.0534$) (Fig. 6K), demonstrating again that the secretome of stimulated ASCs promote the expression of neuronal markers on hNPCs in a higher degree than the regular ASCs secretome.

Discussion

Herein, we developed a device to study electrical stimulation in cell cultures. This device may be particularly important to study cardiac or neurological diseases and to developed innovative therapeutic approaches. Many tissues and organs in the human body experience electrical stimulation as part of their normal physiological function. By mimicking these physiological conditions in vitro, researchers can create more biologically relevant models to study cellular behaviour, tissue development, and disease mechanisms. Moreover, electrical stimulation has been shown to influence cell behavior, including proliferation, differentiation, and maturation. Therefore, these platforms are crucial for tissue engineering applications where researchers aim to guide stem cell differentiation or promote tissue regeneration by providing electrical cues that mimic the natural microenvironment. For these reasons, several approaches to perform in vitro stimulation have been emerged. They differ in the way electric field is applied. For example, it can be constant direct current (DC) field, or different pulse protocols. Applied fields can range in between 10 and 1000 V/m, while pulses can be around milliseconds (ms) and frequencies from 10s of mHz to 100s of Hz [32]. Electrodes can be directly submerged into the culture chamber [23, 24, 33] or they can be interfaced via salt bridges [15, 34]. The first has advantage of simplicity, but with a risks of different electrochemically produced side products and oxidative species affecting the cells. The second option is cleaner, but more complex in the design. For alternating current (AC) stimulation also more complex non-contact capacitive and inductive interfaces are possible, where electrical conductor is even not in direct contact with the culture medium For this exist two approaches: (1) capacitively coupled field [35] and (2) inductive coupling [36, 37]. In case of direct interfacing many different electrodes have been used, such as Pt, Au, Ti, Pt-Ir, ITO [28], various conductive polymers, graphene, carbon [38–40]. Also, electrical driving mechanism can be different based on 2 electrode setups, by current or voltage control and 4-electrode setups. 4-electrode setup offers advantage of more accurate field control, as independent pair of electrodes is used for generating and measuring the signals. However, it is also more complex in implementation compared to the 2-electrode design.

Here we present an in vitro electrical stimulator for multi-well plate. We show it for 12 wells. Similar design has been shown before by Mobini et al. for 6 well [23]. Also commercial stimulator exists by IonOptix for up to 24 wells. IonOptix uses carbon electrodes and Mobini Pt, in our device electrodes were from Pt coated Ti, which has also good electrochemical stability, while being lower in cost. We also report a design of simple and cost-effective stimulation electronics for the system. Designated electronics, such as well-known Grass stimulators are expensive with price about ~ 600USD for single-channel manual device and over 2000USD for more advanced ones. In some examples, such as system shown by Mobini et al. laboratory power supply was used as a voltage source, and all chambers in the multi-well plate were connected in parallel, and thus exposed to the same stimulation protocol [23]. IonOptix C-Pase EM device allows stimulation of 8 different well plates at the same time. All of them use 2-electrode voltage sourcing. This configuration has the advantage that conductivity of the cell culture medium is not important, however due to unknown voltage drop on the electrode and complex interaction of capacitive and Faradaic effects on the electrodes the exact field profile can be difficult to predict and may change over time. Our controller design is simple and modular and could be easily expanded for more channels. We choose to operate stimulation in the constant current mode, in which case the voltage drop on the electrodes would not affect the stimulation field, however it is important to know the conductivity of the culture medium as well as its volume for the accurate field strength.

After the development of the in vitro platform, our investigation focused on the understanding of the effect of electrical stimulation on the neuroblastoma cell line SH-SY5Y. No detrimental effects on the metabolic status of the cells were observed after stimulation. However, it is not clear why S3 settings reduced neurite outgrowth in

SH-SY5Y cells or reduced the number of neurons and the total number of cells in spinal cord mixed cultures. We hypothesize that the specific settings designed to activate spinal neural networks in humans, when directly applied to cells in vitro, may overstimulate the neural cells. This overstimulation could lead to significant ionic imbalances, both intracellularly and extracellularly, potentially triggering excitotoxicity [40]. Additionally, our results demonstrate that ES settings 1 and 2 promote a significant increase in both the number of cells and neurite growth. Subsequently, we extended our analysis to more complex cell cultures, specifically mixed cell cultures of spinal cord. In these cultures, we assessed viability and cell count, and the results mirrored those observed in the SH-SY5Y cell line. Using spinal cord cells, we once again observed that ES promoted neurite outgrowth. Since we observed ES promoted axonal growth in both the SH-SY5Y cell line and in the mixed cell cultures of spinal cord, we suggest that ES promotes constant axonal growth, regardless of the model used. This ES promoted axonal growth was also identified in other studies using different in vitro models, like primary cultures of cortical neurons [41], dorsal root ganglia cultures [42–44], and primary cultures of non-neural cells [45]. Even though, the mechanisms underlying axonal growth after stimulation are still unknown, some possibly correlated mechanisms have been studied, an example is the PI3K/AKT signalling pathway. As observed in our results, Zhong et al. also found an increase in GAP-43 expression, known to be an axonal growth marker. In their study they sought to identify which pathway could be responsible for this increase, concluding that the PI3K/AKT signalling pathway is activated by ES, which in turn induces an increase in GAP-43 expression [41]. Another possibility is the crucial role played by the calcium ion in activating axonal growth associated pathways [43, 44]. In some studies, an increase in calcium ions concentration was reported when ES was applied, leading to the activation of calmodulin-dependent protein kinases (CaMKs), and subsequent phosphorylation of the cAMP response element binding protein (CREB). CREB phosphorylation is then responsible for the transcription of factors like BDNF, a known neurotrophic factor that mediates neuronal development and synaptic function [43, 44, 46]. Previous studies suggest that LTP enhances synaptogenesis and dendritic spine enlargement, both of which are associated with neurite outgrowth. The activity-dependent remodeling characteristic of LTP can also increase synapse density and strengthen local synaptic connections, promoting neurite extension in surrounding areas [47]. It is important to note that inducing LTP typically requires high-frequency stimulation. Among our tested protocols, only the S2 stimulation involved high-frequency stimulation, and we cannot discard that by using low-frequency stimulation on the other ES conditions we may produce a long-term depression [48, 49]. Exploring these possibilities in future studies using our multi-well electrical stimulation platform would be highly interesting.

Herein, we observed no direct correlation between metabolic activity and the total cell number, suggesting that metabolic changes induced by electrical stimulation may not always reflect changes in cell proliferation. Indeed, other authors had previously described that mitochondrial activity measured by MTS can be influenced by factors beyond cell proliferation or viability [50]. We did observe however a significant reduction on the percentage of neurons when applying the stimulation settings S2 and S3, future studies utilizing our in vitro platform should include an evaluation of apoptosis, particularly when working with mixed cell cultures. This would help determine whether electrical stimulation is promoting apoptosis in specific cell populations.

The subsequent phase involved examining the effects of ES in hNPCs. Considering that the S1 protocol was the only one that did not lead to a significant reduction in the percentage of neurons, we decided that the optimal setting for hNPCs was ES1 for 10 min. However, it is important to note that testing different stimulation settings could reveal distinct effects on NPC differentiation, and this would be an interesting focus for future studies. Here, we evaluated the impact of ES on hNPCs with or without the addition of differentiation factors, and it was observed that ES induced greater neurite growth in the absence of differentiation factors. Kobelt et al. [51] also found morphological mature neurons with longer neurite lengths originated upon ES, when compared to no stimulation. Also, an initial neurite retraction upon ES, before the neurite outgrowth was reported. Moreover, in our study, the percentage of MAP-2^{+} cells, a marker for neuronal differentiation, was also higher in the ES group without the addition of differentiation factors when compared to the corresponding control group. In line with our results, Stewart et al. [52] and Tomaskovic-Crook et al. [53] both observed an increase of neurite outgrowth and a higher population of MAP-2 + cells after applying ES, indicating the presence of neuron differentiation. However, the influence of ES seems to be attenuated by the presence of differentiation factors, since greater expression of neuronal markers and neurite outgrowth were not observed when differentiation factors were present. Since the precise mechanism underlying the effects of ES in neuronal cells remain uncertain, and given that even without differentiation factors hNPCs show a large percentage of axonal growth and neuronal maturation when electrically stimulated, associated with an increase of intracellular Ca^{2+} [51], it is thought that the calcium ion fluctuations induced by ES lead to the

activation of important signaling pathways, as previously said [45, 54, 55].

Finally, we extended our exploration to the effects of electrical stimulation on human adult mesenchymal stem cells (MSCs), precisely, adipose stem cells. In this context, we investigated the impact of electrical stimulation on the molecules secreted by ASCs. ASCs are an established cell source for testing therapeutic applications for various diseases. For conditions involving tissues of non-mesodermal origin, the therapeutic effects of ASCs are now understood to primarily arise from their paracrine activity [56]. The secretome—comprising secreted cytokines, growth factors, bioactive lipids, metabolites, and extracellular vesicles—has been studied in preclinical trials for central nervous system disorders, such as spinal cord injury [57–59]. These findings highlight the relevance of studying the effects of electrical stimulation on ASC secretome composition. Herein, ES1 was applied for 30 min to ASCs, followed by an investigation into potential alterations in cell number and morphology. The typical morphology of MSCs, such as ASCs, is spindle-shaped, which corresponds to low circularity. Analyzing the morphology of ASCs can provide insights into their health or differentiation status. For example, ASCs under stress, senescence, or apoptosis tend to adopt a rounder morphology [60], as do ASCs undergoing adipogenic or chondrogenic differentiation [61]. In this study, we observed that electrical stimulation does not alter the normal spindle-shaped morphology of ASCs, suggesting that the applied settings do not induce senescence or differentiation in these cells. Subsequently, the secretome of ASCs was collected and added to hNPCs, with no statistical differences being observed concerning proliferation or survival of the cells. However, the percentage of mature and immature neurons was higher in the electrically stimulated secretome group, showing that the secretome obtained from electrically stimulated ASCs has a significant influence in the expression of neuronal markers on hNPCs. Beugels et al. [62] and Tandon et al. [63] reported an increase in the upregulation of the vascular endothelial growth factor (VEGF) after ES was observed, with Tandon also coming across an increase in the fibroblast growth factor (FGF). These findings confirm what we observed in our study, with the possible increased concentration of growth factors on ASCs secreted proteins explaining the greater percentage of MAP-2^{+} cells found after hNPCs incubation with secretome from electrically stimulated ASCs. On the other hand, analysis to the neurite length demonstrated that the secretome derived from non-stimulated ASCs promoted significantly higher neurite outgrowth than the stimulated secretome. This observation contrasts with studies on electrically stimulated ASCs carried out by Hlavac et al. [64], which reported a significant increase in BDNF concentration in secretome from electrically stimulated ASCs. This discrepancy may highlight the sensitivity of ASCs to specific ES parameters, suggesting that a precise definition of ES parameters could yield a secretome capable of enhancing neurite outgrowth in hNPCs, nevertheless we observed a constant neurite growth across all different cells when stimulated. Interestingly, Cheng et al. [65] and Zhu et al. [66] have not only identified an influence of ES on axonal growth, but also on the fate of NPCs. The latter influence is believed to happen due to the increase in intracellular calcium caused by ES, which will activate different pathways responsible for cell migration, differentiation, and proliferation. Nonetheless, using our specific settings, our findings underscore the context-dependent impact of stimulating ASCs, revealing that the decision to stimulate these cells may prove either beneficial or detrimental, contingent on the specific objective. Specifically, our results indicate that when the goal is to enhance neurite outgrowth, the secretome of non-stimulated ASCs is more suitable. On the other hand, if the objective is to facilitate the differentiation of neural stem cells into new neurons, the secretome derived from electrically stimulated cells may be a preferable choice. These results allow us to suspect that different ES settings possess the ability to alter ASCs secretome, possibly due to the activation of diverse calcium associated signalling pathways. This possibility also influences which type of secretome we should use, since depending on context, objectives, and ES settings the secretome may show different outcomes. It is important to emphasize that in all experiments involving NPCs, further analyses are required to confirm their functional maturation. For instance, electrophysiological recordings, as well as detailed characterization of synaptic and post-synaptic markers, are necessary to determine whether the cells expressing neuronal markers are indeed functional neurons.

It is also important to note that many authors used longer electrical stimulation protocols (1 to 20 h) than the ones used by us [67, 68]. Herein we focused on the effect of short-term ES on cell behavior. Moreover, we did not use serum during the stimulation protocol to prevent potential denaturation of the proteins. Prolonged stimulation in serum-free conditions likely will lead to nutrient deprivation and subsequent cell death. Importantly, we demonstrated that short-term stimulation still resulted in notable outcomes, including enhanced neurite outgrowth, increased neuronal differentiation, and differential effects on the molecules secreted by ASCs. These findings suggest that short periods of electrical stimulation can elicit long-term impacts on the behavior of cells from various origins, underscoring the relevance of studies using short-term electrical stimulation.

Conclusion

Herein we presented a simple and cost-effective platform to stimulate cells in vitro. The characteristics of our stimulator design makes it accessible to a wide range of researchers, including those with limited resources or technical expertise. By providing detailed instructions and using commonly available components, the design facilitates easy reproduction in different laboratory settings, promoting widespread adoption and collaboration across research institutions. Moreover, the flexibility of the design allows for adaptation to various experimental settings and research needs. Researchers can modify parameters such as stimulation frequency, amplitude, and waveform to suit specific experimental requirements or investigate different cellular responses. This adaptability enhances the versatility of the stimulator and its applicability to diverse research applications. This work also allowed us to assess the diverse advantages that the application of electrical stimulation has demonstrated in influencing neuronal and mesenchymal stem cells. Notably, it exhibits the potential to foster axonal growth, increase the expression of neuronal markers on hNPCs, and influence the secretion of factors from ASCs. Designing and developing platforms for electrical stimulation in vitro are essential for advancing our understanding of cellular physiology, disease mechanisms, and therapeutic interventions. These platforms provide researchers with valuable tools for biomedical research.

Abbreviations

AC	Alternating current
ASCs	Adipose Stem Cells
BDNF	Brain-derived neurotrophic factor
bFGF	Basic Fibroblast growth factor
DACs	Digital-to-analog converters
DAPI	4′,6-diamidino-2-phenylindole
DC	Direct current
DCX	Doublecortin
DRGs	Dorsal root ganglions
EC	Electric current
EGF	Epidermal growth factor
ES	Electrical stimulation
FCS	Fetal calf Serum
GAP-43	Growth-associated protein 43
GDNF	Glial cell-line derived neurotrophic factor
GFAP	Glial fibrillary acidic protein
hNPCs	Human Neural Progenitor Cells
MAP-2	Microtubule-associated protein 2
MTS	3-(4,5-Dimethylthiazol-2-yl)-5-(3-carboxymethoxyphenyl)-2-(4-sulfophenyl)-2 H-tetrazolium
NbA	Neurobalsal-A
N-CAM	Neural cell adhesion molecule
NGF	Nerve growth factor
Olig2	Oligodendrocyte transcription factor 2
PBS	Phosphate-buffered saline
PCBs	Printed circuit boards
PFA	Paraformaldehyde
RA	Retinoic acid
RT	Room temperature

Supplementary Information

The online version contains supplementary material available at https://doi.org/10.1186/s42490-025-00090-8.

Supplementary Material 1

Acknowledgements

We would like to acknowledge the support from ICVS and INL through the second edition of the ICVS/INL Hackathon. We would also like to acknowledge the support given by the Portuguese Foundation of Science and Technology to NAS (https://doi.org/10.54499/CEECIND/04794/2017/CP1458/CT0031). We would like to acknowledge the input given by Christian Maibohm, Susana Monteiro, Sara Silva, Eduardo Gomes, Luís Rocha and Madalena Esteves, members of the team that won the second ICVS/INL Hackathon.

Author contributions

JRC: Investigation, Formal analysis, Data curation; MA: Investigation, Formal analysis; MF: Writing – original draft; AV-M: Writing – original draft; JC: Investigation, Formal analysis; TSP: Investigation; AJS: Funding acquisition; AA: Investigation, Formal analysis, Data curation, Methodology, Software, Resources, Validation, Visualization, Conceptualization, Funding acquisition, Writing – original draft, Writing – review & editing; NAS: Data curation, Methodology, Resources, Conceptualization, Funding acquisition, Project administration, Writing – review & editing.

Funding

This work was also funded by "la Caixa" Foundation (LCF/PR/HR23/52430029), by the Santa Casa Neuroscience Awards—Prize Melo e Castro for Spinal Cord Injury Research (MC-18-2021), and by the Wings for Life Spinal Cord Research Foundation (WFL-PT-14/23). Institutional support was also provided by National funds, through the FCT - project UIDB/50026/2020 (https://doi.org/10.54499/UIDB/50026/2020), UIDP/50026/2020 (https://doi.org/10.54499/UIDP/50026/2020) and LA/P/0050/2020 (https://doi.org/10.54499/LA/P/0050/2020).

Data availability

Data is provided within the manuscript or supplementary information files.

Declarations

Ethics approval and consent to participate

All experiments involving animals were approved by the Ethical Subcommittee in Life and Health Sciences Institute (ICVS, Braga, Portugal) and Portuguese Authorities (DGAV; ID:022405). Local regulations on animal care and experimentation (European Union Directive 2010/63/EU) were respected.

Consent for publication

There was no direct involvement of human participants, human samples, or any form of human data use in this work.

Competing interests

The authors declare no competing interests.

Author details

[1]Life and Health Sciences Research Institute (ICVS), School of Medicine, University of Minho, Braga 4710-057, Portugal
[2]ICVS/3B's Associate Lab, PT Government Associated Lab, Braga/Guimarães 4806-909, Portugal
[3]International Iberian Nanotechnology Laboratory (INL), Braga, Portugal

Received: 1 October 2024 / Accepted: 24 February 2025
Published online: 03 March 2025

References

1. Katoh K. Effects of electrical stimulation of the cell: wound healing, cell proliferation, apoptosis, and signal transduction. Med Sci. 2023;11:11. https://doi.org/10.3390/medsci11010011.

2. Huang Y-J, Samorajski J, Kreimer R, Searson PC. The influence of electric field and confinement on cell motility. PLoS ONE. 2013;8:e59447. https://doi.org/10.1371/journal.pone.0059447.
3. Taghian T, Narmoneva DA, Kogan AB. Modulation of cell function by electric field: a high-resolution analysis. J R Soc Interface. 2015;12:20150153. https://doi.org/10.1098/rsif.2015.0153.
4. Zhang XC, Li H. Interplay between the electrostatic membrane potential and conformational changes in membrane proteins. Protein Sci. 2019;28:502–12. https://doi.org/10.1002/pro.3563.
5. Abdul Kadir L, Stacey M, Barrett-Jolley R. Emerging roles of the membrane potential: action beyond the action potential. Front Physiol. 2018;9:1661. https://doi.org/10.3389/fphys.2018.01661.
6. Martínez JM, Delso C, Álvarez I, Raso J. Pulsed electric field-assisted extraction of valuable compounds from microorganisms. Compr Rev Food Sci Food Saf. 2020;19:530–52. https://doi.org/10.1111/1541-4337.12512.
7. Pereda AE, Curti S, Hoge G, Cachope R, Flores CE, Rash JE. Gap junction-mediated electrical transmission: regulatory mechanisms and plasticity. Biochim Biophys Acta BBA - Biomembr. 2013;1828:134–46. https://doi.org/10.1016/j.bbamem.2012.05.026.
8. Schuman EM. Synaptic Transmission in Hippocampal Slice. Methods Neurosci., vol. 31, Elsevier; 1996. pp. 300–8. https://doi.org/10.1016/S1043-9471(96)80029-2
9. Blundon JA, Zakharenko SS. Dissecting the components of Long-Term potentiation. Neurosci Rev J Bringing Neurobiol Neurol Psychiatry. 2008;14:598–608. https://doi.org/10.1177/1073858408320643.
10. Hoare JI, Rajnicek AM, McCaig CD, Barker RN, Wilson HM. Electric fields are novel determinants of human macrophage functions. J Leukoc Biol. 2016;99:1141–51. https://doi.org/10.1189/jlb.3A0815-390R.
11. Yao L, Li Y. The role of direct current electric Field-Guided stem cell migration in neural regeneration. Stem Cell Rev Rep. 2016;12:365–75. https://doi.org/10.1007/s12015-016-9654-8.
12. Li A, Cho J-H, Reid B, Tseng C-C, He L, Tan P, et al. Calcium oscillations coordinate feather mesenchymal cell movement by SHH dependent modulation of gap junction networks. Nat Commun. 2018;9:5377. https://doi.org/10.1038/s41467-018-07661-5.
13. Chang Y-J, Hsu C-M, Lin C-H, Lu MS-C, Chen L. Electrical stimulation promotes nerve growth factor-induced neurite outgrowth and signaling. Biochim Biophys Acta BBA - Gen Subj. 2013;1830:4130–6. https://doi.org/10.1016/j.bbagen.2013.04.007.
14. Ren X, Sun H, Liu J, Guo X, Huang J, Jiang X, et al. Keratinocyte electrotaxis induced by physiological pulsed direct current electric fields. Bioelectrochemistry. 2019;127:113–24. https://doi.org/10.1016/j.bioelechem.2019.02.001.
15. Snyder S, DeJulius C, Willits RK. Electrical stimulation increases random migration of human dermal fibroblasts. Ann Biomed Eng. 2017;45:2049–60. https://doi.org/10.1007/s10439-017-1849-x.
16. Willand MP, Rosa E, Michalski B, Zhang JJ, Gordon T, Fahnestock M, et al. Electrical muscle stimulation elevates intramuscular BDNF and GDNF mRNA following peripheral nerve injury and repair in rats. Neuroscience. 2016;334:93–104. https://doi.org/10.1016/j.neuroscience.2016.07.040.
17. Chen C, Bai X, Ding Y, Lee I-S. Electrical stimulation as a novel tool for regulating cell behavior in tissue engineering. Biomater Res. 2019;23:25. https://doi.org/10.1186/s40824-019-0176-8.
18. Islamov R, Bashirov F, Izmailov A, Fadeev F, Markosyan V, Sokolov M, et al. New therapy for spinal cord injury: autologous Genetically-Enriched leucoconcentrate integrated with epidural electrical stimulation. Cells. 2022;11:144. https://doi.org/10.3390/cells11010144.
19. Silva NA, Madalena CE, Christian M, Eduardo DG, Luis AR, Monteiro S, et al. Dispositivo De Estimulação Elétrica Direta Para Cultura De Células, Método E Aplicações Do Mesmo. Boletim da Propriedade Industrial Nº 2023/05/16, n.d.
20. Baghbaderani BA, Mukhida K, Sen A, Kallos MS, Hong M, Mendez I, et al. Bioreactor expansion of human neural precursor cells in serum-free media retains neurogenic potential. Biotechnol Bioeng. 2010;105:823–33. https://doi.org/10.1002/bit.22590.
21. Dubois SG, Floyd EZ, Zvonic S, Kilroy G, Wu X, Carling S, et al. Isolation of human Adipose-derived stem cells from biopsies and liposuction specimens. In: Prockop DJ, Bunnell BA, Phinney DG, editors. Mesenchymal stem cells. Totowa, NJ: Humana; 2008. pp. 69–79. https://doi.org/10.1007/978-1-60327-169-1_5.
22. Harkema S, Gerasimenko Y, Hodes J, Burdick J, Angeli C, Chen Y, et al. Effect of epidural stimulation of the lumbosacral spinal cord on voluntary movement, standing, and assisted stepping after motor complete paraplegia: a case study. Lancet. 2011;377:1938–47. https://doi.org/10.1016/S0140-6736(11)60547-3.
23. Mobini S, Leppik L, Thottakkattumana Parameswaran V, Barker JH. In vitro effect of direct current electrical stimulation on rat mesenchymal stem cells. PeerJ. 2017;5:e2821. https://doi.org/10.7717/peerj.2821.
24. Akiyama Y, Nakayama A, Nakano S, Amiya R, Hirose J. An electrical stimulation culture system for daily Maintenance-Free muscle tissue production. Cyborg Bionic Syst. 2021;2021(2021/9820505). https://doi.org/10.34133/2021/9820505.
25. C-Dish - IonOptix. n.d. https://www.ionoptix.com/products/components/stimulators/c-dish/ (accessed December 20, 2024).
26. Tandon N, Cannizzaro C, Chao P-HG, Maidhof R, Marsano A, Au HTH, et al. Electrical stimulation systems for cardiac tissue engineering. Nat Protoc. 2009;4:155–73. https://doi.org/10.1038/nprot.2008.183.
27. McCarthy PT, Madangopal R, Otto KJ, Rao MP. Titanium-based multi-channel, micro-electrode array for recording neural signals. 2009 Annu. Int. Conf. IEEE Eng. Med. Biol. Soc., Minneapolis, MN: IEEE; 2009, pp. 2062–5. https://doi.org/10.1109/IEMBS.2009.5334429
28. Silveira C, Brunton E, Escobedo-Cousin E, Gupta G, Whittaker R, O'Neill A, et al. W:Ti flexible transversal electrode array for peripheral nerve stimulation: A feasibility study. IEEE Trans Neural Syst Rehabil Eng. 2020;28:2136–43. https://doi.org/10.1109/TNSRE.2020.3014812.
29. Abdelhak A, Foschi M, Abu-Rumeileh S, Yue JK, D'Anna L, Huss A, et al. Blood GFAP as an emerging biomarker in brain and spinal cord disorders. Nat Rev Neurol. 2022;18:158–72. https://doi.org/10.1038/s41582-021-00616-3.
30. Xu R, Wu C, Tao Y, Yi J, Yang Y, Zhang X, et al. Nestin-positive cells in the spinal cord: a potential source of neural stem cells. Int J Dev Neurosci. 2008;26:813–20. https://doi.org/10.1016/j.ijdevneu.2008.06.002.
31. Messam CA, Hou J, Major EO. Coexpression of Nestin in neural and glial cells in the developing human CNS defined by a human-Specific Anti-nestin antibody. Exp Neurol. 2000;161:585–96. https://doi.org/10.1006/exnr.1999.7319.
32. Li M, Li Z, Wang X, Meng J, Liu X, Wu B, et al. Comprehensive Understanding of the roles of water molecules in aqueous Zn-ion batteries: from electrolytes to electrode materials. Energy Environ Sci. 2021;14:3796–839. https://doi.org/10.1039/D1EE00030F.
33. Zimmermann J, Budde K, Arbeiter N, Molina F, Storch A, Uhrmacher AM, et al. Using a digital twin of an electrical stimulation device to monitor and control the electrical stimulation of cells in vitro. Front Bioeng Biotechnol. 2021;9:765516. https://doi.org/10.3389/fbioe.2021.765516.
34. The Journal of Cell Biology.| JSTOR n.d. https://www.jstor.org/journal/jcellbiology (accessed December 20, 2024).
35. Vaca-González JJ, Guevara JM, Vega JF, Garzón-Alvarado DA. An in vitro chondrocyte electrical stimulation framework: A methodology to calculate electric fields and modulate proliferation, cell death and glycosaminoglycan synthesis. Cell Mol Bioeng. 2016;9:116–26. https://doi.org/10.1007/s12195-015-0419-2.
36. Hess R, Jaeschke A, Neubert H, Hintze V, Moeller S, Schnabelrauch M, et al. Synergistic effect of defined artificial extracellular matrices and pulsed electric fields on osteogenic differentiation of human MSCs. Biomaterials. 2012;33:8975–85. https://doi.org/10.1016/j.biomaterials.2012.08.056.
37. Ahirwar DK, Nasser MW, Jones TH, Sequin EK, West JD, Henthorne TL, et al. Non-contact method for directing electrotaxis. Sci Rep. 2015;5:11005. https://doi.org/10.1038/srep11005.
38. Im C, Seo J-M. A review of electrodes for the electrical brain signal recording. Biomed Eng Lett. 2016;6:104–12. https://doi.org/10.1007/s13534-016-0235-1.
39. Adv Healthcare Materials – 2021. - Zhang - Acridine-Based Covalent Organic Framework Photosensitizer with Broad-Spectrum (1).pdf n.d.
40. Merrill DR, Bikson M, Jefferys JGR. Electrical stimulation of excitable tissue: design of efficacious and safe protocols. J Neurosci Methods. 2005;141:171–98. https://doi.org/10.1016/j.jneumeth.2004.10.020.
41. Zhong H, Xing C, Zhou M, Jia Z, Liu S, Zhu S, et al. Alternating current stimulation promotes neurite outgrowth and plasticity in neurons through activation of the PI3K/AKT signaling pathway. Acta Biochim Biophys Sin. 2023. https://doi.org/10.3724/abbs.2023238.
42. Quan X, Huang L, Yang Y, Ma T, Liu Z, Ge J, et al. Potential mechanism of neurite outgrowth enhanced by electrical stimulation: involvement of MicroRNA-363-5p targeting DCLK1 expression in rat. Neurochem Res. 2017;42:513–25. https://doi.org/10.1007/s11064-016-2100-0.
43. Yan X, Liu J, Huang J, Huang M, He F, Ye Z, et al. Electrical stimulation induces Calcium-Dependent neurite outgrowth and immediate early genes

expressions of dorsal root ganglion neurons. Neurochem Res. 2014;39:129–41. https://doi.org/10.1007/s11064-013-1197-7.
44. Yan X, Liu J, Ye Z, Huang J, He F, Xiao W, et al. CaMKII-Mediated CREB phosphorylation is involved in Ca2+-Induced BDNF mRNA transcription and neurite outgrowth promoted by electrical stimulation. PLoS ONE. 2016;11:e0162784. https://doi.org/10.1371/journal.pone.0162784.
45. Koppes AN, Nordberg AL, Paolillo G, Goodsell N, Darwish H, Zhang L, et al. Electrical stimulation of Schwann cells promotes sustained increases in neurite outgrowth. Tissue Eng Part A 2013:130924230853000. https://doi.org/10.1089/ten.TEA.2013.0012
46. Batty NJ, Fenrich KK, Fouad K. The role of cAMP and its downstream targets in neurite growth in the adult nervous system. Neurosci Lett. 2017;652:56–63. https://doi.org/10.1016/j.neulet.2016.12.033.
47. Harris KM. Structural LTP: from synaptogenesis to regulated synapse enlargement and clustering. Curr Opin Neurobiol. 2020;63:189–97. https://doi.org/10.1016/j.conb.2020.04.009.
48. Shors TJ, Matzel LD. Long-term potentiation: what's learning got to do with it? Behav Brain Sci. 1997;20:597–614. https://doi.org/10.1017/S0140525X97001593.
49. Froc DJ, Chapman CA, Trepel C, Racine RJ. Long-Term depression and depotentiation in the sensorimotor cortex of the freely moving rat. J Neurosci. 2000;20:438–45. https://doi.org/10.1523/JNEUROSCI.20-01-00438.2000.
50. Wang P, Henning SM, Heber D. Limitations of MTT and MTS-Based assays for measurement of antiproliferative activity of green tea polyphenols. PLoS ONE. 2010;5:e10202. https://doi.org/10.1371/journal.pone.0010202.
51. Kobelt LJ, Wilkinson AE, McCormick AM, Willits RK, Leipzig ND. Short duration electrical stimulation to enhance neurite outgrowth and maturation of adult neural stem progenitor cells. Ann Biomed Eng. 2014;42:2164–76. https://doi.org/10.1007/s10439-014-1058-9.
52. Stewart E, Kobayashi NR, Higgins MJ, Quigley AF, Jamali S, Moulton SE, et al. Electrical stimulation using conductive polymer polypyrrole promotes differentiation of human neural stem cells: A biocompatible platform for translational neural tissue engineering. Tissue Eng Part C Methods. 2015;21:385–93. https://doi.org/10.1089/ten.tec.2014.0338.
53. Tomaskovic-Crook E, Zhang P, Ahtiainen A, Kaisvuo H, Lee C-Y, Beirne S, et al. Human neural tissues from neural stem cells using conductive biogel and printed polymer microelectrode arrays for 3D electrical stimulation 2019.
54. Wang M, Li P, Liu M, Song W, Wu Q, Fan Y. Potential protective effect of biphasic electrical stimulation against growth factor-deprived apoptosis on olfactory bulb neural progenitor cells through the brain-derived neurotrophic factor–phosphatidylinositol 3′-kinase/Akt pathway. Exp Biol Med. 2013;238:951–9. https://doi.org/10.1177/1535370213494635.
55. Casalbore P, Barone I, Felsani A, D'Agnano I, Michetti F, Maira G, et al. Neural stem cells modified to express BDNF antagonize trimethyltin-induced neurotoxicity through PI3K/Akt and MAP kinase pathways. J Cell Physiol. 2010;224:710–21. https://doi.org/10.1002/jcp.22170.
56. Pinho AG, Cibrão JR, Silva NA, Monteiro S, Salgado AJ. Cell secretome: basic insights and therapeutic opportunities for CNS disorders. Pharmaceuticals. 2020;13:31. https://doi.org/10.3390/ph13020031.
57. Lentilhas-Graça J. The secretome of macrophages has a differential impact on spinal cord injury recovery according to the polarization protocol. Front Immunol n.d.
58. Assunção-Silva RC, Pinho A, Cibrão JR, Pereira IM, Monteiro S, Silva NA, et al. Adipose tissue derived stem cell secretome induces motor and histological gains after complete spinal cord injury in *Xenopus laevis* and mice. J Tissue Eng. 2024;15:20417314231203824. https://doi.org/10.1177/20417314231203824.
59. Pinho AG, Cibrão JR, Lima R, Gomes ED, Serra SC, Lentilhas-Graça J, et al. Immunomodulatory and regenerative effects of the full and fractioned adipose tissue derived stem cells secretome in spinal cord injury. Exp Neurol. 2022;351:113989. https://doi.org/10.1016/j.expneurol.2022.113989.
60. Govender S, Kruger MJ, Van De Vyver M. Counteracting diabetes-induced adipose tissue derived-stromal cell senescence. Biochimie. 2024;220:11–21. https://doi.org/10.1016/j.biochi.2023.12.001.
61. Campos J, Sampaio-Marques B, Santos D, Barata-Antunes S, Ribeiro M, Serra SC, et al. Lipid priming of adipose mesenchymal stromal cells with docosahexaenoic acid: impact on cell differentiation, senescence and the secretome neuroregulatory profile. Tissue Eng Regen Med 2024. https://doi.org/10.1007/s13770-024-00679-5
62. Beugels J, Molin DGM, Ophelders DRMG, Rutten T, Kessels L, Kloosterboer N, et al. Electrical stimulation promotes the angiogenic potential of adipose-derived stem cells. Sci Rep. 2019;9:12076. https://doi.org/10.1038/s41598-019-48369-w.
63. Tandon N, Goh B, Marsano A, Chao P-HG, Montouri-Sorrentino C, Gimble J, et al. Alignment and elongation of human adipose-derived stem cells in response to direct-current electrical stimulation. 2009 Annu. Int. Conf. IEEE Eng. Med. Biol. Soc., Minneapolis, MN: IEEE; 2009, pp. 6517–21. https://doi.org/10.1109/IEMBS.2009.5333142
64. Hlavac N, Bousalis D, Ahmad RN, Pallack E, Vela A, Li Y, et al. Effects of varied stimulation parameters on Adipose-Derived stem cell response to Low-Level electrical fields. Ann Biomed Eng. 2021;49:3401–11. https://doi.org/10.1007/s10439-021-02875-z.
65. Cheng H, Huang Y, Yue H, Fan Y. Electrical stimulation promotes stem cell neural differentiation in tissue engineering. Stem Cells Int. 2021;2021:1–14. https://doi.org/10.1155/2021/6697574.
66. Zhu R, Sun Z, Li C, Ramakrishna S, Chiu K, He L. Electrical stimulation affects neural stem cell fate and function in vitro. Exp Neurol. 2019;319:112963. https://doi.org/10.1016/j.expneurol.2019.112963.
67. Li Y, Weiss M, Yao L. Directed migration of embryonic stem Cell-derived neural cells in an applied electric field. Stem Cell Rev Rep. 2014;10:653–62. https://doi.org/10.1007/s12015-014-9518-z.
68. Feng J-F, Liu J, Zhang X-Z, Zhang L, Jiang J-Y, Nolta J, et al. Guided migration of neural stem cells derived from human embryonic stem cells by an electric field. Stem Cells. 2012;30:349–55. https://doi.org/10.1002/stem.779.

Publisher's note